

Article

Obtaining Foamed Glass-Ceramics from Diamond Concentration Tailings

Olga V. Suvorova ¹, Nadezhda K. Manakova ¹, Andrey I. Novikov ¹  and Dmitriy V. Makarov ^{2,*}

¹ I.V. Tananaev Institute of Chemistry and Technology of Rare Elements and Mineral Raw Materials, Kola Science Centre of the Russian Academy of Sciences, Fersman St., 26a, Apatity 184209, Russia

² Institute of North Industrial Ecology Problems, Kola Science Centre of the Russian Academy of Sciences, Fersman St., 14a, Apatity 184209, Russia

* Correspondence: mdv_2008@mail.ru; Tel.: +7-81555-79-5-94

Abstract: The possibility of obtaining building foamed glass-ceramic using the diamond concentration tailings of the Lomonosov deposit in Arkhangelsk Region, Russia, is demonstrated here. The effect of the tailings' particle size distribution, feed temperature, the addition of a foaming agent, and the content of oxidizer on the feed charge foaming is established. The process conditions for obtaining foamed glass-ceramic materials are described. The specifications of the materials with the optimal composition (tailings 50 wt.%, glass waste 50 wt.%, SiC 0.5 wt.%, Fe₂O₃ 1 wt.%) foamed at 1020–1050 °C were as follows: apparent density 0.23–0.51 g/cm³, compression strength 0.58–2.40 MPa, water absorption (by volume) 8.7–19.0%. Based on the combination of the measured properties when used in dry conditions, the obtained materials can be considered heat-insulating foam materials. The thermal conductivity was 0.060–0.066 W/m·K.

Keywords: foamed glass-ceramics; diamond concentration tailings; waste glass; apparent density; compressive strength; water absorption; thermal conductivity



Citation: Suvorova, O.V.; Manakova, N.K.; Novikov, A.I.; Makarov, D.V. Obtaining Foamed Glass-Ceramics from Diamond Concentration Tailings. *Ceramics* **2023**, *6*, 1139–1151. <https://doi.org/10.3390/ceramics6020068>

Academic Editor: Enrico Bernardi

Received: 1 February 2023

Revised: 4 May 2023

Accepted: 10 May 2023

Published: 18 May 2023



Copyright: © 2023 by the authors. Licensee MDPI, Basel, Switzerland. This article is an open access article distributed under the terms and conditions of the Creative Commons Attribution (CC BY) license (<https://creativecommons.org/licenses/by/4.0/>).

1. Introduction

The government strategy for the development of the building materials industry for the period through 2030, enacted by the Government of the Russian Federation (Order 868-r dated on 10 May 2016 [1]), emphasizes that the main trends in the global building materials industry in recent years have been:

- A transition to a new level of energy efficiency of production;
- A reduction in the negative impact on the environment;
- The involvement of waste in the production of building materials and increasing the processing depth of natural resources;
- The production of new types (innovative and composite) of building materials that improve energy efficiency, reliability, durability, and internal environment quality in buildings and structures and reduce material consumption.

The European Construction Technology Platform (ECTP) sets out more specific requirements, not only for building materials and their properties, but also for the respective manufacturing processes and construction technology using such materials. According to the ECTP, by 2030 the following key performance indicators are to be achieved in the global construction industry: a 30% reduction in the energy intensity of producers of building materials, a 30% reduction in the amount of natural resources consumed in the production of such materials, a 30% reduction in the life cycle cost of buildings, a 50% reduction in occupational injuries in the construction industry, a 40% reduction in construction industry waste generation, and up to 99% construction waste recycling (no more than 1% to be deposited at waste dumps) [2]. For successful development in the directions proposed by

these strategic documents, new tools for implementing the principles of energy-efficient construction are needed.

Due to its geographical location and harsh climatic conditions, Russia is forced to spend huge amounts of energy on heating buildings and structures. In addition, the energy problem involves the low quality and limited range of materials used for the thermal insulation of heat generating installations, heat supply lines and facilities [3]. It is specifically in regions with harsh natural and climatic conditions that heat-insulating materials are in high demand in the first place.

The use of natural and secondary mineral resources is expected to expand the resource base of the building materials industry and contribute to the development of principles for obtaining new foamed materials with improved properties [4].

This applies, in particular, to diamond mining operations, responsible for the formation of significant volumes of overburden, with kimberlite concentration tailings stored in tailing dumps occupying large areas. In Russia's Arkhangelsk Region, this type of waste is represented by the tailings formed during the concentration of kimberlite pipe from the Lomonosov deposit operated by Severalmaz Joint-stock Company (JSC). Up to 1 million tons of watery, sandy argillaceous rock is annually deposited in the tailing dump [5,6].

The Institute of Comprehensive Exploitation of Mineral Resources of the Russian Academy of Sciences has developed an efficient electrochemical method for desliming the recycled water of the tailings storage facility at Severalmaz JSC, with the recovery of a saponite-containing product [5]. The use of electrochemically modified saponite to obtain high-quality ceramic building materials with improved physical, mechanical, and aesthetic properties provided higher compressive (by a factor of 1.4–1.7) and bending (by a factor of 1.3–3.3) strengths compared to materials derived from the original product. The strength properties of the samples (compressive strength from 35 to 80.9 MPa, bending strength from 8 to 26.7 MPa) in the firing temperature ranged from 800 to 1000 °C, matching those of the high-grade M300 ceramic bricks [6].

To build upon this development, we initiated research into the feasibility of processing (recycling) the coarser sand fraction of the tailings, deposited in the tailings storage facility beach zone, for the production of foamed glass-ceramics.

Foamed glass-ceramics are sintered building materials with low thermal conductivity (0.05–0.1 W/m·K), characterized by closed micropores up to 8 µm in diameter. The main source materials used in the production of building ceramic foams are clays, diatomites, siliceous minerals, alkaline geopolymers, etc.

The use of mining and metallurgical industry waste for the production of foamed materials is discussed in a number of studies; [4,7–19], etc. Note, however, that the main process obstacles to the disposal of these wastes are the instability of their properties, the presence of impurities, and the inadequate knowledge of the physicochemical processes that occur during the heat treatment of the feeds. A resource- and energy-saving process for obtaining the heat-insulating material "Siver" with a density of less than 150 kg/m³ based on the silica gel, a fluorosalt by-product, was proposed in [20]. In [21], another promising process was discussed—the low-temperature synthesis of glass foamed heat-insulating materials based on phosphate ore processing waste. In [22,23], the copper-zinc ore concentration tailings of the Zhezkazgan deposit in Kazakhstan were studied as a feedstock for obtaining a granular material similar to foam glass, using a low-temperature process without complete melting of the feed. Chinese researchers used purified glass from cathode ray tubes and panels obtained during the dismantling of TV sets, as well as germanium-containing concentration tailings, to obtain high-strength porous foamed glass-ceramic materials [24]. Ceramic foamed materials were obtained from waste glass wool and spodumene tailings, mainly consisting of quartz feldspar sand [25]. Fly ash from thermal power plants, alumina red mud, and concentration tailings were used to synthesize foamed ceramics [26–29]. A number of studies have examined the applications of metallurgical slags [30,31], etc. For example, in [30] foamed glass was obtained with a powder process using broken glass and titanium-containing blast-furnace slag with Na₂B₄O₇·5H₂O as a

flux. Foamed glass-ceramic materials derived from blast-furnace slag and glass waste were obtained in [31]. For the formation of nuclei of crystalline phases, TiO_2 , ZrO_2 , and CaF_2 were used.

Obtaining various types of foamed glass is one of the promising areas for glasses' waste recycling. The main difficulty is the heterogeneity of glass in terms of chemical composition, which affects the stability of the recycling process and the quality of the finished product. Multiple publications are devoted to the use of glass waste in the production of foamed materials, including glazing glass, medical glass, and glass containers [32–39]. Progress has been made in the disposal of the so-called waste monitor glass found in the cathode-ray tubes of TV receivers, computer monitors, etc. [40]. This has been successfully processed into both block and granular foamed glass products [41–45].

A number of papers have been devoted to the mechanism of charge foaming based on cullet (soda–lime–silicate glass) using various foaming agents (SiC , Si_3N_4 , AlN). In some cases, additional oxidizers have been used to intensify foam formation, for example MnO_2 , Fe_2O_3 , and CeO_2 , leading to a more uniform microstructure compared to carbide or nitride foam agents used separately [46–48].

The demand for effective heat-insulating materials and the availability of significant quantities of overburden, and concentration tailings occupying large storage areas, dictate the need to develop process flows for producing new foam materials with improved properties. The purpose of this study was to evaluate the possibility of obtaining building glass-ceramic foam materials using the diamond concentration tailings of the Lomonosov deposit in the Arkhangelsk Region of Russia. The effects were established on the particle size distribution of the tailings, the sintering temperature, the presence of a foaming agent, and the content of an oxidizing agent on the foaming of the feed charge.

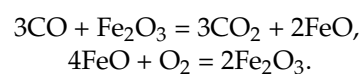
2. Materials and Methods

The feasibility of obtaining foamed glass-ceramics from the sand fraction of the concentration tailings of processing plant no. 1 of Severalmaz JSC (hereinafter referred to as tailings) was examined. For these purposes, we used an average process sample of 12 kg of dry residue, from which the <0.63 mm fraction was isolated and reground to <0.05 mm. The tailings were a red-brown powder with a specific surface area of $11.93 \text{ m}^2/\text{g}$ and a bulk density of $655 \text{ kg}/\text{m}^3$. Part of the experiments was carried out with a fraction of $<0.63 >0.05$ mm.

Glass waste (crushing window and bottle glass) was used to improve the sintering process of the ceramic matrix. Chemical composition of waste, wt.%: SiO_2 74.1, Al_2O_3 1.6, Fe_2O_3 0.1, CaO 10.1, MgO 1.6, $\text{Na}_2\text{O} + \text{K}_2\text{O}$ 12.3, SO_3 0.2. The presence of flux led to an increase in the amount of liquid phase at a lower temperature, which contributed to the compaction of the structure of the surface shell of the ceramic matrix and locked the formed gas inside the material structure. Waste glass ground to a size of <0.05 mm with a bulk density of $660 \text{ kg}/\text{m}^3$ was used.

In the production of foamed glass-ceramics, silicon carbide (Grade 63 C, GOST R 52381-2005) was used as a foaming agent, contributing to the production of foamed materials with a porous matrix structure.

Simultaneously with the gasifier for the complete oxidation of SiC , Grade OSCh 2–4 Fe_2O_3 was added. With the participation of iron oxide, reactions with gaseous carbon monoxide are possible, proceeding with insignificant heat absorption:



The composition, structure, and properties of the raw source and produced materials were studied using a combination of methods. The specific surface area (S_{sp}) of the source materials was measured by the BET method using nitrogen sorption/desorption isotherms and a TriStar II 3020 V.1.03 instrument. The particle size distribution was established using a SALD-201V particle size analyzer.

X-ray diffraction analysis (XRD) was performed on a Shimadzu XRD 6000 diffractometer (Kyoto, Japan) and $\text{CuK}\alpha$ radiation. X-ray images were taken with an increment of 0.02° (2θ), and the signal accumulation time at each point was 1 s. Thermal gravimetric-differential scanning calorimeter (TG-DSC) analysis was performed using a STA409 PC Luxx NETZSCH instrument (Selb, Germany) in an argon atmosphere at a heating rate of $10^\circ\text{C}/\text{min}$. Heating was carried out in the temperature range of $20\text{--}1300^\circ\text{C}$. The study of feed swelling was carried out using a high-temperature optical microscope ZEISS MHO-2 (Oberkochen, Germany).

The thermophysical properties of foamed glass-ceramics were determined and evaluated based on the requirements of GOST 17177-94 (heat-insulating building materials and products; test methods) and GOST 16381-77 (heat-insulating building materials and products; classification and general specifications).

The apparent density ρ (g/cm^3) of a sample was measured as the ratio of its mass to volume:

$$\rho = m/V,$$

where m is the mass of the dried sample, g; V is the volume of the sample, cm^3 .

The apparent density was taken as the arithmetic mean of the density measurements of all samples, calculated to $0.02 \text{ g}/\text{cm}^3$.

Water absorption ($W, \%$) by volume was calculated using the following formula:

$$W = \frac{(m_1 - m)}{V\rho_w} \times 100,$$

where m_1 is the mass of the sample after saturation with water, g; m is the mass of the sample, previously dried to a constant mass, g; V is the volume of the sample, cm^3 ; and ρ_w is the density of water, g/cm^3 . Water absorption was measured as the arithmetic mean of a series of tests of individual samples (5–10 samples). The test was carried out until the results of two successive measurements differed by no more than 0.1%.

The porosity ($P, \%$) of the samples was estimated based on the pre-determined values of true and average density according to the following formula:

$$P = \left(1 - \frac{\rho_{av}}{\rho_t}\right) \times 100,$$

where ρ_{av} is the average density, g/cm^3 , and ρ_t is the true density of the sample, g/cm^3 .

Tests of foamed glass-ceramics for compressive strength were carried out using a PGM-100MG hydraulic press (Russia) on cylinder samples, provided that the height and diameter of the sample were equal ($20 \pm 2 \text{ mm}$). The ultimate compressive strength (R_{comp} , MPa) of the sample was calculated by the formula:

$$R_{comp} = F/S_{av},$$

where F is the breaking load, N, and S_{av} is the area to which the load was applied, cm^2 .

The essence of the method was to create a stationary heat flux passing through a flat sample of a certain thickness and directed perpendicular to the front faces of the sample, measuring the sample thickness, heat flux density, and temperature of the opposite front faces. The thickness of the measured sample was 18–20 mm. To determine the thermal conductivity coefficient, an electronic thermal conductivity meter ITP-MG 4 (Russia) was used. The thermal conductivity λ (effective thermal conductivity) was estimated using the formula:

$$\lambda = \frac{H \cdot q}{T_H - T_x},$$

where λ is the effective thermal conductivity, $\text{W}/\text{m}\cdot\text{K}$; H is the thickness of the measured sample, mm; q is the density of the stationary heat flux passing through the measured

sample, W/m^2 ; T_H is the temperature of the hot face of the measured sample, K; and T_X is the temperature of the cold face of the measured sample, K.

3. Results and Discussion

The XRD data of the powder used in foamed glass-ceramics production are shown in Figure 1. The diffraction pattern shows an amorphous halo and reflections of crystalline phases, mainly related to quartz, dolomite, and calcite. Small quantities of an iron mineral, herzenite, were present.

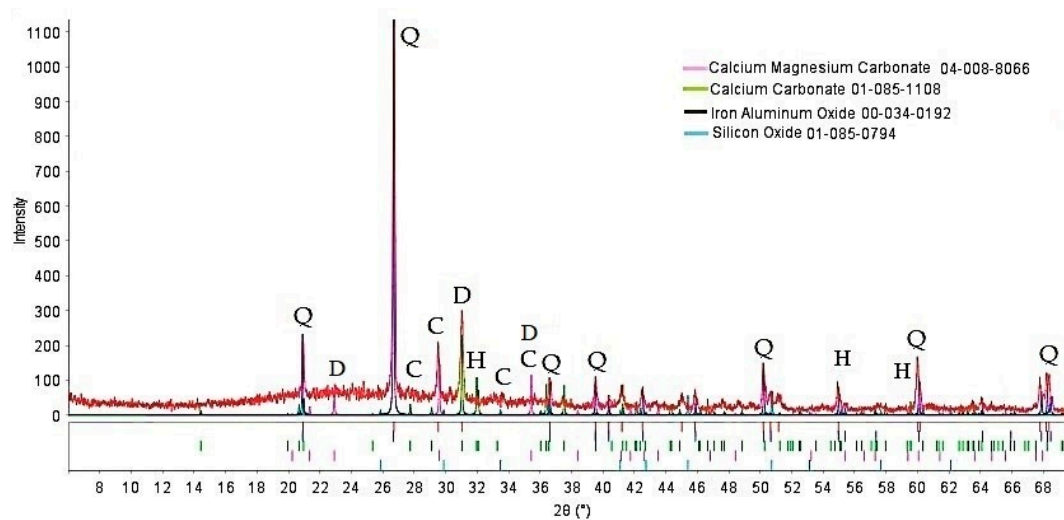


Figure 1. XRD pattern of the tailings. Q—quartz, C—calcite, D—dolomite, H—herzenite.

The chemical composition of the tailings is presented in Table 1. In accordance with the feed specifications for the production of building materials, including ceramics and ceramic foams, when using waste the charge composition needs to be modified, for example, with waste glass. The chemical composition of the waste glass was as follows, wt.%: SiO_2 74.1, Al_2O_3 1.6, Fe_2O_3 0.1, CaO 10.1, MgO 1.6, $Na_2O + K_2O$ 12.3, SO_3 0.2.

Table 1. Feed specifications in the production of building materials.

Composition of Feed	Diamond Concentration Tailings	Clay Material for the Production of Expanded Clay Gravel, Crushed Stone, Sand, etc. (GOST 32026-2012)	Building Ceramics (GOST 32026-2012)
Average composition, wt.%			
$Na_2O + K_2O$	0.49	1.5–6.0	
Silicon dioxide SiO_2	49.95	No more than 70	53.0–81.0
Al_2O_3	2.30	7.0–25.0	7.0–23.0
CaO	11.41	Max 6.0	
MgO	7.35	No more than 4.0	
MnO	0.32		
SO_3	-	No more than 2.0	No more than 2.0
$Fe_2O_3 + FeO$	4.82	2.5–12.0	2.5–8.0
TiO_2	0.63	0.1–2.0	
P_2O_5	0.30		
LOI	16.20		

Due to the fact that the fineness of the feed materials has a significant impact on the quality and properties of foamed glass-ceramics, the particle size distribution range of ground tailings was established (Figure 2).

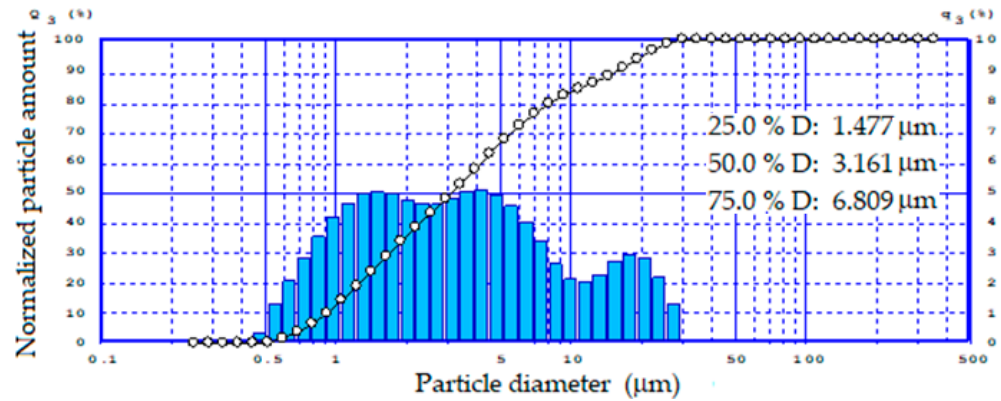


Figure 2. Particle size distribution of the tailings.

According to the data obtained, the reground tailings had a relatively narrow bimodal particle size distribution from 0.5 to 35 μm .

The results of the TG-DSC analysis of the tailings sample are presented in Figure 3.

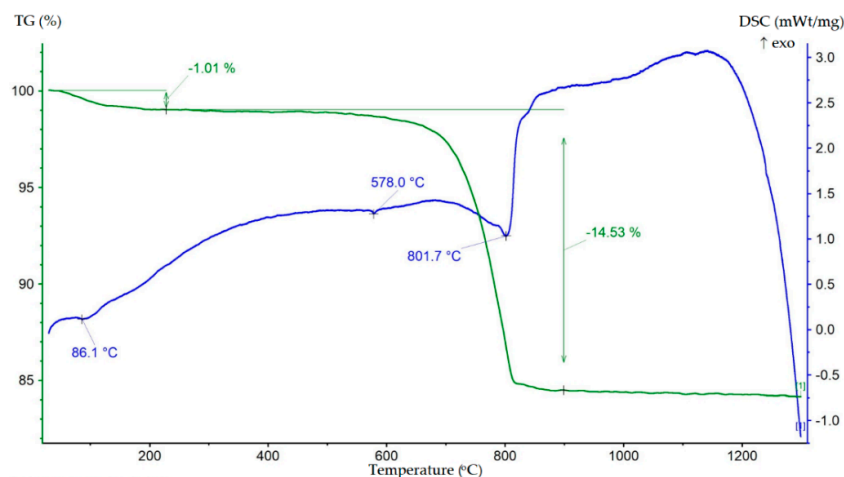


Figure 3. TG–DSC result of the tailings sample.

The DSC data showed two main endothermic effects. The first was a low-intensity endothermic effect with a peak at 86.1 $^{\circ}\text{C}$, accompanied by a change in mass by 1.01%, associated with the release of adsorbed water. The second, more intense endothermic effect, in the temperature range 700–900 $^{\circ}\text{C}$ with a minimum at 801.7 $^{\circ}\text{C}$, was related to the decarbonization of dolomite and the dissociation of calcite, as evidenced by a mass change of 14.53%. A minor endothermic effect with a minimum at 578 $^{\circ}\text{C}$ was associated with the reversible polymorphic transformation of α -quartz into β -quartz. It can be noted that the TG-DSC data were in agreement with the XRD.

Preliminarily, as part of an exploratory experiment to determine the possibility of obtaining foamed glass-ceramics, the foaming process of samples of different compositions was studied using a microscope analysis. Samples for testing were prepared as follows. Feed materials of a certain composition were thoroughly mixed. Water was added as a binder in an amount of 5–8 wt.%. Cubic samples with an edge length of 3 mm were prepared in a mold, placed on a corundum substrate, and moved to a furnace. Sintering was carried out up to the temperature of the size increase in the sample, and then with an increment of 50–100 $^{\circ}\text{C}$, with an analysis conducted at each maximum temperature.

The effects of various factors on the foaming process, such as the particle size distribution of the powder, the heating temperature of the charge, the presence of a foaming agent, and the content of the oxidizing agent, were established.

Tailings of two sizes were used in the experiments: $<0.63 >0.05$ mm (samples 1 to 8) and < 0.05 mm (samples 9 to 26).

At the first stage, experiments were carried out on the tailings without additives and with the addition of 30 wt.% of waste glass, which demonstrated insufficient foaming of the feed. Samples were heated to 1100 °C. Considering this, 50% wt.% of waste glass, a foaming agent, and an oxidizing agent (Fe_2O_3) were added to the charge.

The compositions of the charges, foaming conditions, and properties of the samples after heat treatment are presented in Table 2. For each composition, three samples were prepared.

Table 2. Foaming tests using high-temperature microscope MHO-2.

Sample	Starting Temperature of Sample Size Increase, °C	Sintering Temperature, °C	Foaming Ratio	Sample Properties after Heat Treatment
Tailings ($<0.63 >0.05$ mm) 50 wt.% – Waste glass 50 wt.%				
1	800	800	1.30	Bulk sintering, increase in size.
2		900	1.30	Sintering, increase in size, open porosity.
3		1000	1.40	Surface melting, swelling, ball shape.
4		1100	1.33	Surface melting, gaseous phase breakthrough, ball shape.
Tailings ($<0.63 >0.05$ mm) 50 wt.% – Waste glass 50 wt.% + SiC 0.5 wt.% (over 100 wt.%)				
5	840	800	1.30	Sintering, increase in size, open porosity.
6		900	1.50	Increase in size, surface melting, gaseous phase breakthrough, ball shape.
7		1000	1.40	Increase in size, surface melting, minor gaseous phase breakthrough, ball shape.
8		1100	1.30	Increase in size, surface melting, gas phase breakthrough, brittle, ball shape.
Tailings (<0.05 mm) 50 wt.% – Waste glass 50 wt.% + SiC 0.5 wt.% (over 100 wt.%)				
9	780	800	1.25	Sintering, increase in size, cubic shape.
10		900	1.30	Sintering, increase in size, cubic shape.
11		1000	1.55	Surface melting, increase in size, gaseous phase breakthrough, ball shape.
12		1100	1.50	Surface melting, increase in size, minor gaseous phase breakthrough, ball shape.
Tailings (<0.05 mm) 50 wt.% – Waste glass 50 wt.% + SiC 0.5 wt.% (over 100 wt.%) + Fe_2O_3 1 wt.% (over 100 wt.%)				

Table 2. Cont.

Sample	Starting Temperature of Sample Size Increase, °C	Sintering Temperature, °C	Foaming Ratio	Sample Properties after Heat Treatment
13	800	950	1.20	Sintering, slight increase in size.
14		1000	1.20	Initial surface melting, slight increase in size, cubic shape.
15		1050	1.35	Surface melting, swelling, minor gaseous phase breakthrough, ball shape.
16		1100	1.60	Surface melting, swelling, ball shape.
Tailings (<0.05 mm) 50 wt.% – Waste glass 50 wt.% + SiC 0.5 wt.% (over 100 wt.%) + Fe ₂ O ₃ 3 wt.% (over 100 wt.%)				
17	840	800	1.26	Sintering, slight increase in size, cubic shape.
18		900	1.20	Sintering, slight increase in size, cubic shape.
19		950	1.25	Slight melting, increase in size, cubic shape.
20		970	1.30	Surface melting, swelling, ball shape.
21		1000	1.59	Surface melting, swelling, minor gaseous phase breakthrough, ball shape.
22		1050	1.65	Surface melting, swelling, minor gaseous phase breakthrough, ball shape.
Tailings (<0.05 mm) 50 wt.% – Waste glass 50 wt.% + SiC 0.5 wt.% (over 100 wt.%) + Fe ₂ O ₃ 5 wt.% (over 100 wt.%)				
23	880	900	1.20	Sintering, slight increase in size, cubic shape.
24		1000	1.20	Sintering, slight increase in size, cubic shape.
25		1050	1.30	Slight melting, hemispheric shape.
26		1100	1.30	Slight melting, ball shape.

From the data presented in Table 2, it can be seen that the foaming of the samples was the strongest when using a fine fraction of the feed. The introduction of an additional foaming agent into the charge contributed to a noticeable increase in the size of the sample and an improvement in its structure (pore distribution and size). Iron oxide, introduced in a dispersed state into the charge, slightly reduced its foaming capacity, which is consistent with the findings in [49], but contributed to a more ordered structure of the material. More efficient gas formation with a higher quality of the outer surface was demonstrated by samples with iron-containing additives at 1 wt.% (samples 13 to 16) and 3 wt.% (samples 17 to 22).

It was established that all samples of the studied compositions had a relatively low foaming ratio not higher than 1.65, which is explained by the high content of the residual crystalline phase in the material. The highest foaming ratio was exhibited by finely ground feed with the addition of 3 wt.% Fe₂O₃ (sample 22), which was probably due to the formation of a sufficient amount of glass phase, the temperature match of gas formation, and more complete oxidation of the SiC.

Subsequently, to study the foaming of a charge based on the tailings and to obtain foam materials, tailings sized < 0.05 mm, SiC as a foaming agent at 0.5 wt.%, and Fe₂O₃ as an oxidant at 1, 2, 3 and 5 wt.% were used.

For the manufacture of foamed glass-ceramics, the feed charge was thoroughly homogenized, loaded into split ceramic cylinder molds, and lubricated with a suspension based on a mixture of chalk and corundum. The prepared molds with the charge were loaded into a “Nabertherm” electric furnace (Germany) for sintering (foaming) in the temperature range 900–1100 °C at an exposure time of 10–50 min at maximum temperature. The charge was loaded into a cold furnace and heated to the foaming temperature. Since the best performance in terms of foaming and lower density was demonstrated by samples placed in a furnace preheated to a given temperature, further experiments were carried out in this way. After foaming, annealing was carried out, i.e., an arbitrary decrease in temperature to ambient temperature (cooling in a furnace), for 15–20 h.

The properties of the resulting material were evaluated according to the following criteria: apparent density, compressive strength, water absorption, thermal conductivity, and macrostructure of the samples.

Key properties of the foamed glass-ceramics composed of 50 wt.% tailings, 50 wt.% waste glass, 0.5 wt.% SiC, and 1 wt.% Fe₂O₃ are presented in Table 3.

Table 3. Physical and mechanical properties of foam glass ceramics.

Sintering Temperature, °C	Apparent Density, g/cm ³	Porosity, %	Compressive Strength, MPa	Water Absorption, % (by Volume)	Thermal Conductivity, W/m·K
1020	0.51 ± 0.02	77.1 ± 0.08	2.40 ± 0.05	8.7 ± 0.17	0.060 ± 0.004
1030	0.28 ± 0.02	88.3 ± 0.09	1.20 ± 0.02	9.5 ± 0.19	0.066 ± 0.005
1040	0.25 ± 0.02	84.9 ± 0.09	1.05 ± 0.02	12.8 ± 0.26	0.062 ± 0.004
1050	0.23 ± 0.02	91.3 ± 0.09	0.58 ± 0.01	19.0 ± 0.38	0.061 ± 0.004

A preliminary study of the physical and mechanical properties of the samples of the above composition foamed at 1020–1050 °C showed that the apparent density of the material was 0.23–0.51 g/cm³, the compressive strength 0.58–2.40 MPa, and the water absorption (by volume) 8.7–19.0%. The samples had a rather low thermal conductivity of 0.060–0.066 W/m·K, matching that of foam glass.

To improve the performance and primarily reduce water absorption by the foamed glass-ceramics, the composition of the initial charge and process conditions needed to be adjusted, which required further research.

In the XRD pattern of samples sintered at temperatures of 1020–1050 °C, the presence of a glass phase, as well as diopside, quartz, and cristobalite, was noted. An increase in the halo intensity in the angle range of 15–35°, along with the sintering temperature, indicated an increase in the content of the glass phase. With an increase in temperature, an increase in the diopside reflections intensity was observed as well as a decrease in the quartz and cristobalite peaks intensity (Figure 4).

As is known, in order to obtain foamed glass-ceramics with improved performance, a uniform finely porous structure is required. The macrostructure of the samples foamed at different temperatures is shown in Figure 5. An analysis of the micrographs showed that the structure of the foamed glass-ceramics depended on temperature. Samples obtained at a temperature of 1020 °C were characterized by a finely porous structure (Figure 6a,b) with randomly located pores with a size of 0.16–2.67 mm. The structure of the foamed glass-ceramics obtained at a temperature of 1030 °C approached the optimum. The presence of evenly distributed polydisperse (in size) pores, which were separated by dense and similar cross-section interpore partitions, was recorded. As can be seen from Figure 6c,d, the pore structure was represented by cells 1.29–3.87 mm in size, predominantly close to a round shape, remotely resembling a honeycomb structure in appearance. Such a space–volume configuration is the most optimal for foamed glass-ceramics capable of being resistant to sufficiently large loads at a minimum density value. The thickness of the interpore partition

in the sample was 0.14–1.16 mm. At a temperature of 1040 °C, an increase in the number of larger pores of 4.37–5.60 mm in size was observed (Figure 6e,f). An increase in temperature to 1050 °C led to a change in porosity towards the predominance of large pores with an average size of 6.70–8.00 mm (Figure 6g,h). The presence of single pores up to 10 mm in size is possible. Increasing the sintering temperature leads to enlarged pores and the breakthrough of the gaseous phase as a result of a decrease in the viscosity and surface tension of the melt. Such a structure is not optimal, which is confirmed by an increase in water absorption, as well as a decrease in the material strength. At the same time, with an increase in the sintering temperature of 30 °C, water absorption increases by a factor of 2.1.

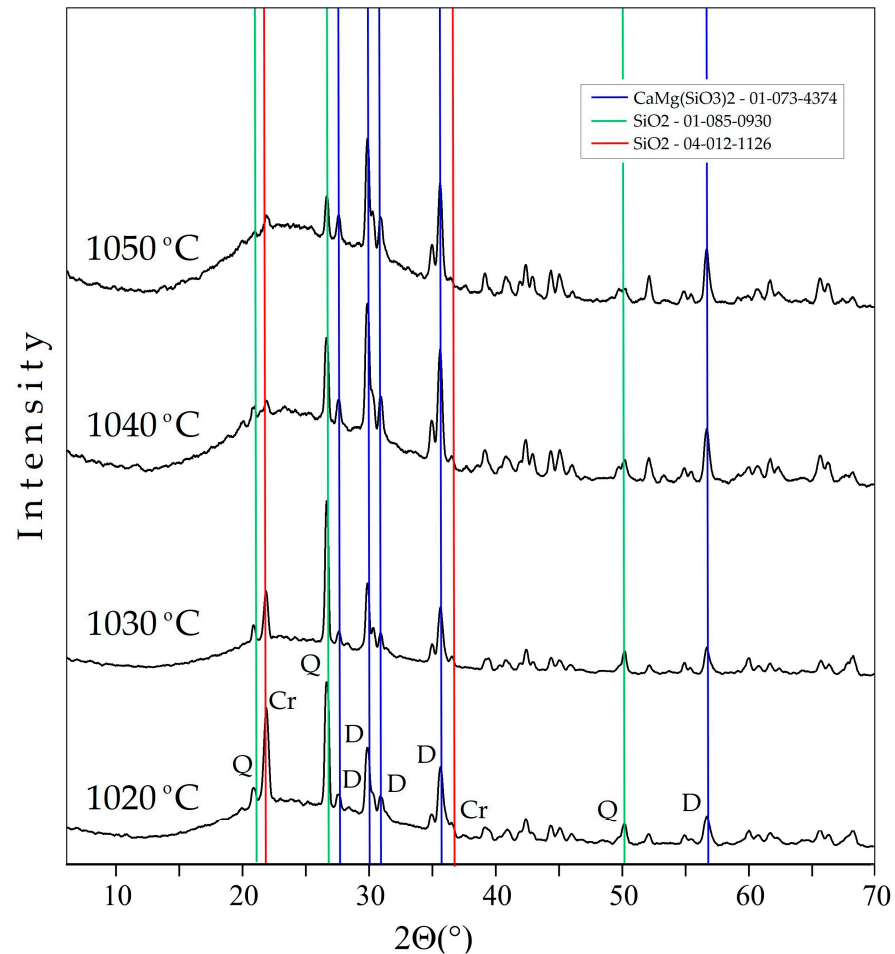


Figure 4. XRD patterns of foamed glass-ceramics sintered at temperatures of 1020–1050 °C. D—diopside, Q—quartz, Cr—cristobalite.

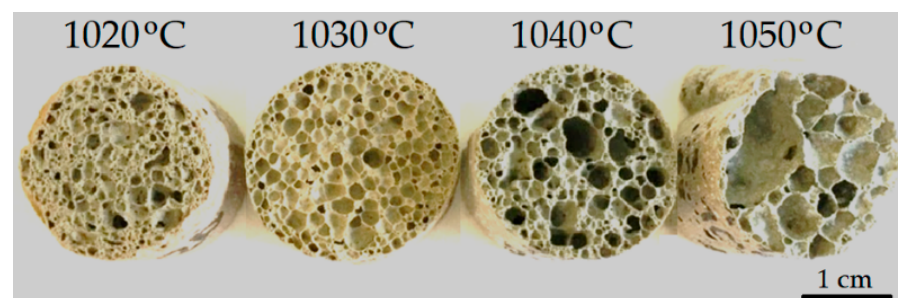


Figure 5. Macrostructures of the samples foamed at different temperatures.

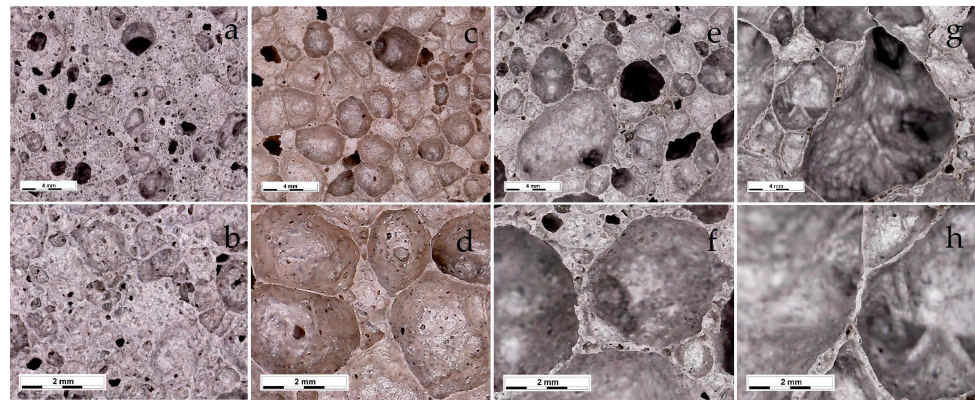


Figure 6. Microstructures of the samples foamed at different temperatures: 1020 °C (a,b); 1030 °C (c,d); 1040 °C (e,f); 1050 °C (g,h).

The results obtained showed that the optimal sintering temperature was 1030 °C. Samples of the described composition, obtained at the indicated temperature, were the closest to the specifications for glass-ceramic foams. The exception was the increased water absorption, the reduction of which requires further research.

4. Conclusions

1. The feasibility was demonstrated of diamond processing tailings of the Lomonosov deposit in the Arkhangelsk Region, Russia, into building foamed glass-ceramics.
2. The effects on the foaming process of the feed charge of the particle size distribution of the tailings, the heating temperature, the presence of a foaming agent, and the content of an oxidizer were established. The results indicate that it is advisable to use a fine fraction of the feed materials (-0.05 mm) and introduce SiC as a foaming agent and Fe_2O_3 as an oxidizer into the charge to improve sintering up to waste glass. The optimal process conditions for obtaining foamed glass-ceramics were identified.
3. Materials were obtained that possessed a relatively low thermal conductivity of $0.060\text{--}0.066$ W/m·K, which allowed these to be classified as heat-insulating. The best properties in terms of apparent density, compressive strength, porosity, pore shape and distribution were demonstrated by the following charge, wt.%: tailings 50, waste glass 50, SiC 0.5, Fe_2O_3 1 at a sintering temperature of 1030 °C and an exposure time of 30 min. The samples were characterized by apparent density 0.28 ± 0.02 g/cm³, compression strength 1.20 ± 0.02 MPa, and water absorption (by volume) $9.5 \pm 0.19\%$.
4. Our findings are expected to form the basis of the development of processes for the production of innovative building materials that will improve the energy efficiency, reliability, and durability of buildings and structures. The recycling of industrial waste will help to reduce the environmental footprint.

Author Contributions: Conceptualization, O.V.S., N.K.M. and D.V.M.; Methodology, O.V.S., N.K.M. and D.V.M.; Investigation, O.V.S., N.K.M., A.I.N. and D.V.M.; Writing—Original Draft Preparation, O.V.S., N.K.M., A.I.N. and D.V.M.; Writing—Review and Editing, O.V.S., N.K.M. and D.V.M.; Visualization, O.V.S., N.K.M., A.I.N. and D.V.M. All authors have read and agreed to the published version of the manuscript.

Funding: This research was funded by the Russian Government, grants no. FMEZ-2022-0018 and FMEZ-2022-0010.

Institutional Review Board Statement: Not applicable.

Informed Consent Statement: Not applicable.

Data Availability Statement: The data presented in this study are available upon request from the corresponding author after obtaining the permission of an authorized person.

Conflicts of Interest: The authors declare no conflict of interest.

References

1. Order 868-r of the Government of the Russian Federation dated 10 May 2016 (as Amended on 23 November 2016) “On the Strategy for the Development of the Building Materials Industry for the Period through 2020 and Long-Term Prospects through 2030”. Available online: http://www.consultant.ru/document/cons_doc_LAW_197766/ (accessed on 18 January 2023).
2. Strategy for the Innovative Development of the Construction Industry in the Russian Federation for the Period through 2030. Available online: https://www.minstroyrf.gov.ru/docs/?date_from=&t%5B%5D=&d%5B%5D=&q=%D0%A1%D1%82%D1%80%D0%B0%D1%82%D0%B5%D0%B3%D0%B8%D1%8F&active%5B%5D=65&active%5B%5D=66 (accessed on 17 May 2023). (In Russian)
3. Lotov, V.A. Making foam glass based on natural and technogenic aluminosilicates. *Glass Ceram.* **2012**, *68*, 302–305. [[CrossRef](#)]
4. Suvorova, O.V.; Manakova, N.K.; Makarov, D.V. Use of bulk industrial wastes in the production of glass foam materials. *Glass Ceram.* **2021**, *77*, 384–389. [[CrossRef](#)]
5. Minenko, V.G. Justification and design of electrochemical recovery of saponite from recycled water. *J. Mining Sci.* **2014**, *50*, 595–600. [[CrossRef](#)]
6. Chanturiya, V.; Minenko, V.; Suvorova, O.; Pletneva, V.; Makarov, D. Electrochemical modification of saponite for manufacture of ceramic building materials. *Appl. Clay Sci.* **2017**, *135*, 199–205. [[CrossRef](#)]
7. Rawlings, R.D.; Wu, J.P.; Boccaccini, A.R. Glass-ceramics: Their production from wastes—A Review. *J. Mater. Sci.* **2006**, *41*, 733–761. [[CrossRef](#)]
8. Ponsot, I.; Bernardo, E. Self glazed glass ceramic foams from metallurgical slag and recycled glass. *J. Clean. Prod.* **2013**, *59*, 245–250. [[CrossRef](#)]
9. Luo, Y.; Zheng, S.; Ma, S.; Liu, C.; Wang, X. Preparation of sintered foamed ceramics derived entirely from coal fly ash. *Constr. Build. Mater.* **2018**, *163*, 529–538. [[CrossRef](#)]
10. Xi, C.; Zheng, F.; Xu, J.; Yang, W.; Peng, Y.; Li, Y.; Li, P.; Zhen, Q.; Bashir, S.; Liu, J.L. Preparation of glass-ceramic foams using extracted titanium tailing and glass waste as raw materials. *Constr. Build. Mater.* **2018**, *190*, 896–909. [[CrossRef](#)]
11. Chen, Z.; Wang, H.; Ji, R.; Liu, L.; Cheeseman, C.; Wang, X. Reuse of mineral wool waste and recycled glass in ceramic foams. *Ceram. Int.* **2019**, *45*, 15057–15064. [[CrossRef](#)]
12. Min’ko, N.I.; Puchka, O.V.; Stepanova, M.S.; Vaysera, S.S. *Heat-Insulating Glass Materials: Foam Glass, Izd*; BGTU: Belgorod, Russia, 2016; 262p. (In Russian)
13. Suvorova, O.V.; Makarov, D.V.; Pletneva, V.E. Ceramic materials based on tailings from enrichment of vermiculite and apatite-nepheline ores. *Glass Ceram.* **2009**, *66*, 255–257. [[CrossRef](#)]
14. Manakova, N.K.; Suvorova, O.V. Heat-insulating material on the basis of silica-containing wastes formed in crude ore recovery in Kola Peninsula. *Rus. J. App. Chem.* **2012**, *85*, 1654–1657. [[CrossRef](#)]
15. Kazmina, O.V.; Tokareva, A.Y.; Vereshchagin, V.I. Using quartzofeldspathic waste to obtain foamed glass material. *Res-Eff. Technol.* **2016**, *2*, 23–29.
16. Manakova, N.K.; Suvorova, O.V.; Makarov, D.V. Influence of mineral additives on the structure and properties of heat-insulating materials based on silica-containing raw material. *Glass Ceram.* **2021**, *78*, 328–332. [[CrossRef](#)]
17. Makarov, D.V.; Manakova, N.K.; Suvorova, O.V. Production of rock-based foam-glass materials (review). *Glass Ceram.* **2023**, *79*, 411–417. [[CrossRef](#)]
18. Manakova, N.K.; Suvorova, O.V.; Semushin, V.V. Physicochemical substantiation of obtaining porous glass materials from silica-containing raw materials. *Glass Phys. Chem.* **2023**, *49*, 193–198.
19. Spiridonov, Y.A.; Orlova, L.A. Problems of foam glass production. *Glass Ceram.* **2003**, *60*, 313–314. [[CrossRef](#)]
20. Tereshchenko, I.M.; Zhikh, B.P.; Kravchuk, A.P. Production of efficient heat-insulating materials on the basis of silica gel. *Build. Mater.* **2016**, *7*, 45–48. (In Russian)
21. Tereshchenko, I.M.; Dormeshkin, O.B.; Kravchuk, A.P.; Zhikh, B.P. Status and prospects of development of production of gassy foamed heat-insulation materials. *Glass Ceram.* **2017**, *74*, 216–219. [[CrossRef](#)]
22. Tokareva, A.Y. Study of copper-zinc ore dressing tailings as a raw material for producing foam glass. In *Chemistry and Chemical Technology in the 21st Century*; Tomsk Polytechnic University: Tomsk, Russia, 2016; pp. 127–128. (In Russian)
23. Kazmina, O.V.; Semke, A.P.; Miskovets, A.Y. Preparation of porous glass ceramics on the basis of copper-zinc ore dressing wastes. In *Problems of Geology and Development of Mineral Resources*; Tomsk Polytechnic University: Tomsk, Russia, 2017; Volume 2, pp. 374–375. (In Russian)
24. Zhang, Q.; He, F.; Shu, H.; Qiao, Y.; Mei, S.; Jin, M.; Xie, J. Preparation of high strength glass ceramic foams from waste cathode ray tube and germanium tailings. *Constr. Build. Mater.* **2016**, *111*, 105–110. [[CrossRef](#)]
25. Lemougna, P.N.; Yliniemi, J.; Adediran, A.; Luukkonen, T.; Tanskanen, P.; Finnil, M.; Illikainen, M. Synthesis and characterization of porous ceramics from spodumene tailings and waste glass wool. *Ceram. Int.* **2021**, *47*, 33286–33297. [[CrossRef](#)]
26. Chen, X.; Lu, A.; Qu, G. Preparation and characterization of foam ceramics from red mud and fly ash using sodium silicate as foaming agent. *Ceram. Int.* **2013**, *39*, 1923–1929. [[CrossRef](#)]
27. Guo, Y.; Zhangn, Y.; Huangn, H.; Meng, K.; Hu, K.; Hu, P.; Wang, X.; Zhang, Z.; Meng, X. Novel glass ceramic foams materials based on red mud. *Ceram. Int.* **2014**, *40*, 6677–6683. [[CrossRef](#)]

28. Liu, T.; Lin, C.; Liu, J.; Han, L.; Gui, H.; Li, C.; Zhou, X.; Tang, H.; Yang, Q.; Lu, A. Phase evolution, pore morphology and microstructure of glass ceramic foams derived from tailings wastes. *Ceram. Int.* **2018**, *44*, 14393–14400. [[CrossRef](#)]
29. Xia, F.; Cui, S.; Pu, X. Performance study of foam ceramics prepared by direct foaming method using red mud and K-feldspar washed waste. *Ceram. Int.* **2022**, *48*, 5197–5203. [[CrossRef](#)]
30. Wang, H.; Feng, K.; Zhou, Y.; Sun, Q.; Shi, H. Effects of $\text{Na}_2\text{B}_4\text{O}_7 \cdot 5\text{H}_2\text{O}$ on the properties of foam glass from waste glass and titania-bearing blast furnace slag. *Mater. Lett.* **2014**, *132*, 176–178. [[CrossRef](#)]
31. Ding, L.; Ning, W.; Wang, Q.; Shi, D.; Luo, L. Preparation and characterization of glass-ceramic foams from blast furnace slag and waste glass. *Mater. Lett.* **2015**, *141*, 327–329. [[CrossRef](#)]
32. Heriyanto; Pahlevani, F.; Sahajwalla, V. From waste glass to building materials An innovative sustainable solution for waste glass. *J. Clean. Prod.* **2018**, *191*, 192–206. [[CrossRef](#)]
33. Ducman, V.; Kovačević, M. The foaming of waste glass. *Key Eng. Mater.* **1997**, *132–136*, 2264–2267. [[CrossRef](#)]
34. Fernandes, H.R.; Tulyaganov, D.U.; Ferreira, J.M.F. Production and characterization of glass ceramic foams from recycled raw materials. *Adv. Appl. Ceram.* **2009**, *108*, 9–13. [[CrossRef](#)]
35. Vancea, C.; Lazău, I. Glass foam from window panes and bottle glass wastes. *Centr. Eur. J. Chem.* **2014**, *12*, 804–811. [[CrossRef](#)]
36. Bernardo, E.; Scarinci, G.; Bertuzzi, P.; Ercole, P.; Ramon, L. Recycling of waste glasses into partially crystallized glass foams. *J. Porous. Mater.* **2010**, *17*, 359–365. [[CrossRef](#)]
37. Abbasi, S.; Mirkazemi, S.M.; Ziaee, A.; Saeedi Heydari, M. The Effects of Fe_2O_3 and Co_3O_4 on Microstructure and properties of foam glass from soda lime waste glasses. *Glass. Phys. Chem.* **2014**, *40*, 173–179. [[CrossRef](#)]
38. Dragoescu, M.F.; Paunescu, L.; Axinte, S.M.; Fiti, A. Influence of the color of bottle glass waste on the characteristics of foam glass produced in microwave field. *Int. J. Sci. Eng. Inv.* **2018**, *7*, 95–100.
39. Attila, Y.; Güden, M.; Taşdemirci, A. Foam glass processing using a polishing glass powder residue. *Ceram. Int.* **2013**, *39*, 5869–5877. [[CrossRef](#)]
40. Ciftci, M.; Cicek, B. E-waste: A review of CRT (cathode ray tube) recycling. *J. Mater. Sci.* **2017**, *5*, 1–17. [[CrossRef](#)]
41. Guo, H.W.; Gong, Y.X.; Gao, S.Y. Preparation of high strength foam glass-ceramics from waste cathode ray tube. *Mater. Lett.* **2010**, *64*, 997–999. [[CrossRef](#)]
42. Lee, C.-T. Production of alumino-borosilicate foamed glass body from waste LCD glass. *J. Ind. Eng. Chem.* **2013**, *19*, 1916–1925. [[CrossRef](#)]
43. Fernandes, H.; Andreola, F.; Barbieri, L.; Lancellotti, I.; Pascual, M.J.; Ferreira, J.M.F. The use of egg shells to produce cathode ray tube glass foams. *Ceram. Int.* **2013**, *39*, 9071–9078. [[CrossRef](#)]
44. Petersen, R.R.; König, J.; Smedskjaer, M.M.; Yue, Y. Effect of Na_2CO_3 as foaming agent on dynamics and structure of foam glass melts. *J. Non-Cryst. Sol.* **2014**, *400*, 1–5. [[CrossRef](#)]
45. Mucsi, G.; Csúke, B.; Kertész, M.; Hoffmann, L. Physical characteristics and technology of glass foam from waste cathode ray tube glass. *J. Mater.* **2013**, *2013*, 1–11. [[CrossRef](#)]
46. Bernardo, E.; Cedro, R.; Florean, M.; Hreglich, S. Reutilization and stabilization of wastes by the production of glass foams. *Ceram. Int.* **2007**, *33*, 963–968. [[CrossRef](#)]
47. Saburit, A.; Orts, M.J.; Garcia-Ten, J.; Bernardo, E.; Colombo, P. Foaming of flat glass cullet using Si_3N_4 and MnO_2 powders. *Ceram. Int.* **2009**, *35*, 1953–1959.
48. García-Ten, J.; Saburit, A.; Orts, M.J.; Bernardo, E.; Colombo, P. Glass foams from oxidation/reduction reactions using SiC , Si_3N_4 and AlN powders. *Glass Technol. Eur. J. of Glass Sci. Technol. Part A.* **2011**, *52*, 103–110.
49. Dushkina, M.A.; Kazmina, O.V. Effect of iron-containing additives on the process of obtaining foam glass crystalline materials. *Chem. Chem. Technol.* **2014**, *57*, 54–57.

Disclaimer/Publisher’s Note: The statements, opinions and data contained in all publications are solely those of the individual author(s) and contributor(s) and not of MDPI and/or the editor(s). MDPI and/or the editor(s) disclaim responsibility for any injury to people or property resulting from any ideas, methods, instructions or products referred to in the content.